Inorg. Chem. **2009**, *48*, 2456−2463

Copper(II) Dinuclear Pyrazine-Based Rack-Type Complexes: Preparation, Structure, and Magnetic Properties

Juan Ramírez,[†] Adrian-Mihail Stadler,[†] Guillaume Rogez,[‡] Marc Drillon,*[,‡] and Jean-Marie Lehn*[,†]

Laboratoire de Chimie Supramoléculaire, Institut de Science et d'Ingénierie Supramoléculaires, Université de Strasbourg, 8 allée Gaspard Monge, Strasbourg, 67083, France, and Institut de Physique et Chimie des Matériaux de Strasbourg, UMR CNRS-ULP 7504, Groupe des Matériaux Inorganiques, 23 rue du Loess, BP43, 67034 Strasbourg cedex 2, France

Received September 4, 2008

A novel class of ditopic ligands, **1**, was synthesized by the reaction of 2,5-pyrazine-dicarboxaldehyde with 2 equiv of acyl-/aroyl-hydrazine. Their structures were confirmed by 1D and 2D NMR and by X-ray crystallography. They gave heteroleptic Cu(II) dinuclear rack-like complexes of the formula $[Cu_2\mathbf{1}(terpy)_2](OTf)_4$, thus undergoing shape changes of significant amplitude. The solid-state structures of these complexes were determined by X-ray crystallography. The magnetic measurements performed on the complexes revealed the presence of antiferromagnetic intramolecular interactions.

Introduction

Rack-like complexes are polynuclear heteroleptic complexes containing one polytopic backbone ligand coordinating several metal ions that are, each of them, in addition coordinated by one or more ligands. Such architectures bringing together a more or less linear sequence of metal ions are interesting for their physical properties[1−3] or as synthetic precursors for larger architectures.[4a,b] Few examples are reported in the literature: Ru(II) racks,[1,2] Cu(I) racks,[4a,b] or Zn(II) racks with phenanthroline-based ditopic ligands[4c] and Eu(III), La(III), or Y(III) rack-like complexes.[3]

Pyrazine was employed in coordination chemistry as a bismonodentate ligand,[5] but the pyrazine unit was also included in polydentate[6] ligands. Thanks to its two N atoms in the

* To whom correspondence should be addressed. E-mail: Marc.Drillon@ipcms.u-strasbg.fr (M.D.), lehn@isis.u-strasbg.fr (J.-M.L.).
[†] Université de Strasbourg.
[‡] Institut de Physique et Chimie des Matériaux de Strasbourg.

(1) (a) Stadler, A.-M.; Puntoriero, F.; Campagna, S.; Kyritsakas, N.; Welter, R.; Lehn, J.-M. *Chem.—Eur. J.* **2005**, *11*, 3997–4009. (b) Loiseau, F.; Nastasi, F.; Stadler, A.-M.; Campagna, S.; Lehn, J.-M. *Angew. Chem., Int. Ed.* **2007**, *46* (32), 6144–6147.
(2) (a) Hanan, G. S.; Arana, C. R.; Lehn, J.-M.; Fenske, D. *Angew. Chem.* **1995**, *107*, 1191; *Angew. Chem., Int. Ed.* **1995**, *34* 1122−1124. (b) Hanan, G. S.; Arana, C. R.; Lehn, J.-M.; Baum, G.; Fenske, D. *Chem.—Eur. J.* **1996**, *2*, 1292–1302. (c) Hasenknopf, B.; Hall, J.; Lehn, J.-M.; Balzani, V.; Credi, A.; Campagna, S. *New J. Chem.* **1996**, *20*, 725–730. (d) Ceroni, P.; Credi, A.; Balzani, V.; Campagna, S.; Hanan, G. S.; Arana, C. R.; Lehn, J.-M. *Eur. J. Inorg. Chem.* **1999**, *9*, 1409–1414. (e) Brown, D.; Muranjan, S.; Jang, Y.; Thummel, R. *Org. Lett.* **2002**, *4*, 1253–1256. (f) Brown, D.; Zong, R.; Thummel, R. P. *Eur. J. Inorg. Chem.* **2004**, *3269*, 3272. (g) For related Ru(II) complexes used for water oxidation, see: Zong, R.; Thummel, R. P. *J. Am. Chem. Soc.* **2005**, *127*, 12802–12803.
(3) Castano-Briones, M. M.; Bassett, A. P.; Meason, L. L.; Ashton, P. R.; Pikramenou, Z. *Chem. Commun.* **2004**, 2832−2833.
(4) (a) Schmittel, M.; Kalsani, V.; Bats, J. W. *Inorg. Chem.* **2005**, *44*, 4115–4117. (b) Kalsani, V.; Bodenstedt, H.; Fenske, D.; Schmittel, M. *Eur. J. Inorg. Chem.* **2005**, *1841*, 1849. (c) Schmittel, M.; Kalsani, V.; Kishore, R. S. K.; Cölfen, H.; Bats, J. W. *J. Am. Chem. Soc.* **2005**, *127*, 11544–11545.
(5) (a) Haddad, M. S.; Hendrickson, D. N.; Cannady, J. P.; Drago, R. S.; Bieksza, D. S. *J. Am. Chem. Soc.* **1979**, *101* (4), 898–906. (b) Julve, M.; Verdaguer, M.; Faus, J.; Tinti, F.; Moratal, J.; Monge, A.; Gutierrez-Puebla, E. *Inorg. Chem.* **1987**, *26*, 3520–3527. (c) Das, A.; Todorov, I.; Dey, S. K.; Mitra, S. *Inorg. Chim. Acta* **2006**, *359*, 2041–2046. (d) Woodward, F. M.; Gibson, P. J.; Jameson, G. B.; Landee, C P.; Turnbull, M. M.; Willett, R. D. *Inorg. Chem.* **2007**, *46* (10), 4256–4266. (e) Jeβ, I.; Taborsky, P.; Pospíšil, J.; Näther, C. *Dalton Trans.* **2007**, *2263*, 2270.
(6) For Cu(II) complexes with pyrazine-based ligands, see:(a) Fleischer, E. B.; Lawson, M. B. *Inorg. Chem.* **1972**, *11*, 2772–2775. (b) Fleischer, E. B.; Jeter, D.; Florian, R. *Inorg. Chem.* **1974**, *13*, 1042–1047. (c) O'Connor, C. J.; Klein, C. L.; Majeste, R. J.; Trefonas, L. M. *Inorg. Chem.* **1982**, *21* (1), 64–67. (d) Oshio, H.; Nagashima, U. *Inorg. Chem.* **1990**, *29*, 3321–3325. (e) Neels, A.; Stoeckli-Evans, H.; Escuer, A.; Vicente, R. *Inorg. Chim. Acta* **1997**, *260*, 189–198. (f) Grove, H.; Julve, M.; Lloret, F.; Kruger, P. E.; Törnroos, K. W.; Slettene, J. *Inorg. Chim. Acta* **2001**, *325*, 115–124. (g) Grove, H.; Sletten, J.; Julve, M.; Lloret, F. *J. Chem. Soc., Dalton Trans.* **2001**, *2487*, 2493. (h) Hausmann, J.; Jameson, G. B.; Brooker, S. *Chem. Commun* **2003**, *2992*, 2993. (i) Carranza, J.; Grove, H.; Sletten, J.; Lloret, F.; Julve, M.; Kruger, P. E.; Eller, C.; Rillema, D. P. *Eur. J. Inorg. Chem.* **2004**, *4836*, 4848. (j) Sun, Y.-Q.; Zhang, J.; Chen, J.-L.; Yang, G.-Y. *Eur. J. Inorg. Chem.* **2004**, *3837*, 3841. (k) Beobide, G.; Castillo, O.; Luque, A.; Garcia-Couceiro, U.; Garcia-Teran, J. P.; Roman, P. *Inorg. Chem.* **2006**, *45* (14), 5367–5382. (l) Ismayilov, R. H.; Wang, W.-Z.; Lee, G.-H.; Wang, R.-R.; Liu, I. P.-C.; Yeh, C.-Y.; Peng, S.-M. *Dalton Trans.* **2007**, *27*, 2898–2907.

10.1021/ic801675d CCC: $40.75
Published on Web 02/09/2009

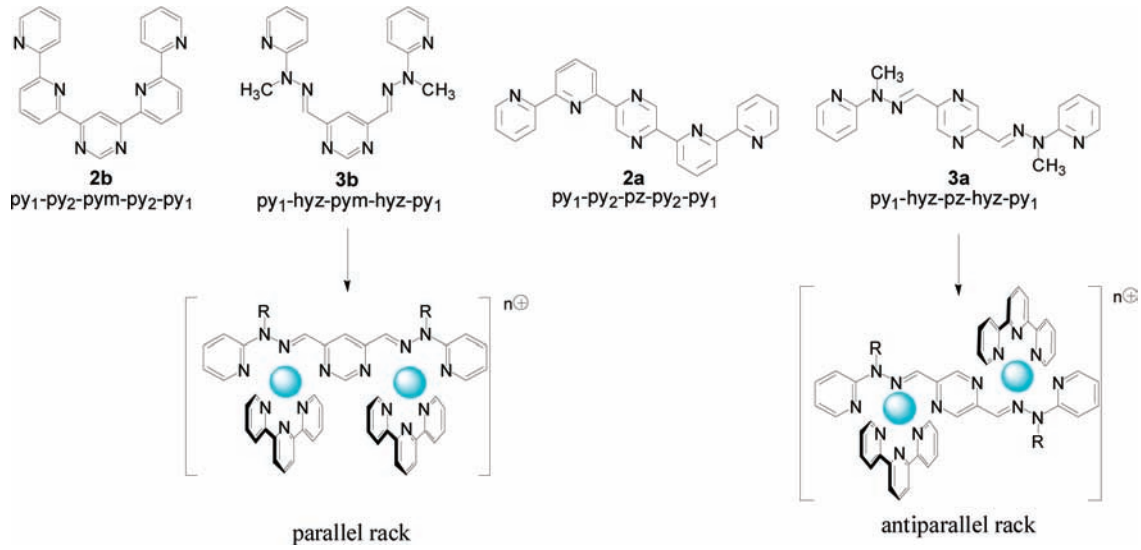

Figure 1. Structures of ligands $py_1-py_2-pym/pz-py_2-py_1$ (**2**) and $py_1-hyz-pym/pz-hyz-py_1$ (**3**) and of the two types of rack complexes: "parallel" pyrimidine-based and "antiparallel" pyrazine-based racks.

para position, it often acts as a bridging ligand. Using the 2,5-disubstituted pyrazine as a central unit in ditopic ligands leads to antiparallel rack-like complexes.

In our laboratories, hydrazone-based analogues of $py_1-py_2-pym-py_2-py_1$ligand[7]**2b** (py_1 = 2-substituted-pyridine, py_2 = 2,6-disubstituted-pyridine, pym = 4,6-disubstituted pyrimidine) were synthesized by replacing the py_2 unit with an isomorphic equivalent, the hydrazone group (hyz):[8] $py_1-hyz-pym-hyz-py_1$, **3b** (Figure 1). A similar synthetic method was employed to conceive and obtain hydrazone-based analogue $py_1-hyz-pz-hyz-py_1$, **3a**,[1] of the pyrazine-based ligand $py_1-py_2-pz-py_2-py_1$, **2a**,[9] with a 2,5-disubstituted-pyrazine (pz) as a central unit (Figure 1). The general synthetic strategy[1a] consists of the condensation of the pyrazine-2,5-dicarboxaldehyde[10] with a hydrazine or a hydrazide.[11] Bis(acyl-/aroyl-hydrazone ligands), **1** (Schemes 1 and 2), of this last category are a novel, unexplored class of ditopic ligands.

With respect to the relative orientation of the two coordination subunits presented by the coordinated ditopic backbone ligand of a dinuclear rack, two types of isomeric racks may be generated:

• The "parallel" one, that has a plane of symmetry perpendicular to the plane of the backbone ligand and where the subunits are oriented in the same direction, as in pyrimidine-derived backbone ligands.

• The "antiparallel" one, that has a C_2 axis perpendicular to the plane of the backbone ligand and where the subunits are oriented in opposite directions, as in pyrazine-based backbone ligands (Figure 1).

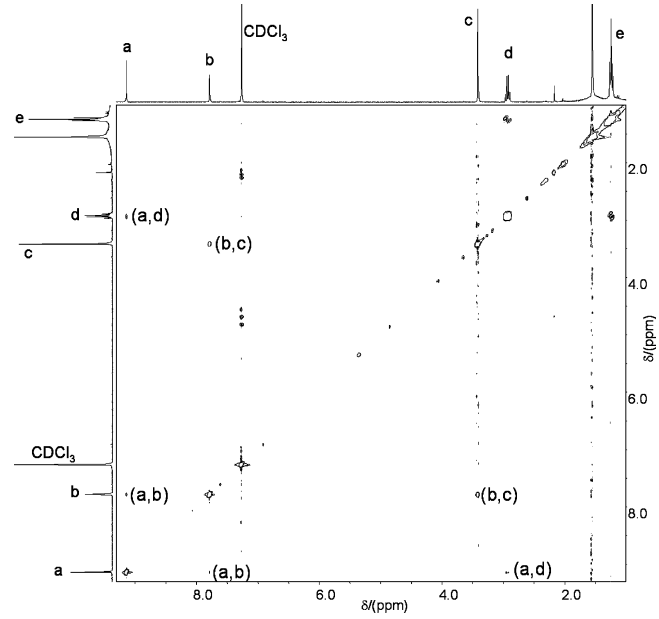

Figure 2. $^1H-^1H$ NOESY spectrum of ligand **1a** (300 MHz, $CDCl_3$).

In such complexes, the two metal ions are in proximity, thus making possible the existence of superexchange metal−metal interactions mediated by the bridging ring (pym or pz). The nature of the bridging ring (pym or pz) should have influence on the metal−metal interaction.

We report here on the synthesis, structure, and properties of the "antiparallel" rack-type heteroleptic complexes formed by Cu(II) ions with 2,2′;6,2″-terpyridine (terpy) and the ditopic bis-tridentate ligands **1** incorporating 2,5-disubstituted pyrazine (Scheme 1).

(7) (a) Hanan, G. S.; Lehn, J.-M.; Kyritsakas, N.; Fischer, J. *J. Chem. Soc., Chem. Commun.* **1995**, 765−766. (b) Bassani, D. M.; Lehn, J.-M.; Baum, G.; Fenske, D. *Angew. Chem.* **1997**, *109*, 1931−1933; *Angew. Chem., Int. Ed.* **1997**, *36*, 1845−1847. (c) Ohkita, M.; Lehn, J.-M.; Baum, G.; Fenske, D. *Chem.—Eur. J.* **1999**, *5*, 3471–3481.

(8) (a) Gardinier, K. M.; Khoury, R. G.; Lehn, J.-M. *Chem.—Eur. J.* **2000**, *6*, 4124–4131. (b) Schmitt, J.-L.; Stadler, A.-M.; Kyritsakas, N.; Lehn, J.-M. *Helv. Chim. Acta* **2003**, *86*, 1598–1624. (c) Stadler, A.-M.; Kyritsakas, N.; Graff, R.; Lehn, J.-M. *Chem.—Eur. J.* **2006**, *12*, 4503.

(9) (a) Bark, T.; Düggeli, M.; Stoeckli-Evans, H.; von Zelewsky, A. *Angew. Chem.* **2001**, *113*, 2924; *Angew. Chem., Int. Ed.* **2001**, *40*, 2848. (b) Bark, T.; Stoeckli-Evans, H.; von Zelewsky, A. *J. Chem. Soc., Perkin Trans. 1*, **2002**, *1881*.

(10) (a) Wiley, R. H. *J. Macromol. Sci. Chem.* **1987**, *A24*, 1183. (b) Wiley, R H. U.S. Paternt 4,260,757, 1981.

(11) For pyrimidine based ligands, see: Cao, X.-Y.; Harrowfield, J.; Nitschke, J.; Ramírez, J.; Stadler, A.-M.; Kyritsakas-Gruber, N.; Madalan, A.; Rissanen, K.; Russo, L.; Vaughan, G.; Lehn, J.-M. *Eur. J. Inorg. Chem.* **2007**, *2944*, 2965.

Scheme 1. Synthesis of Complexes **9** = $[Cu_2\mathbf{1}(terpy)_2](OTf)_4$

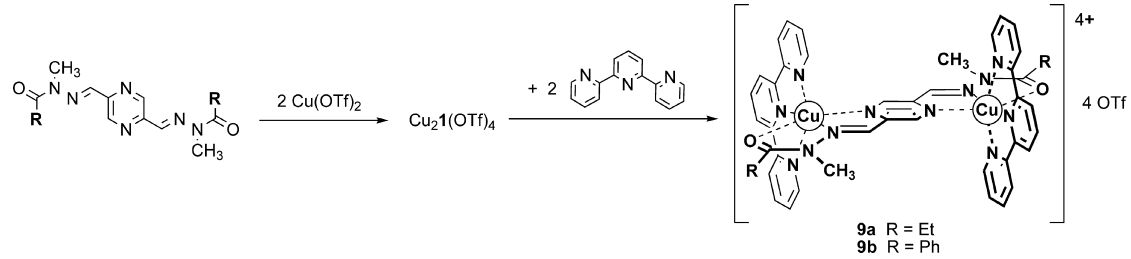

Scheme 2. Synthesis of the Pyrazine-Based Ligands **1a** and **1b**

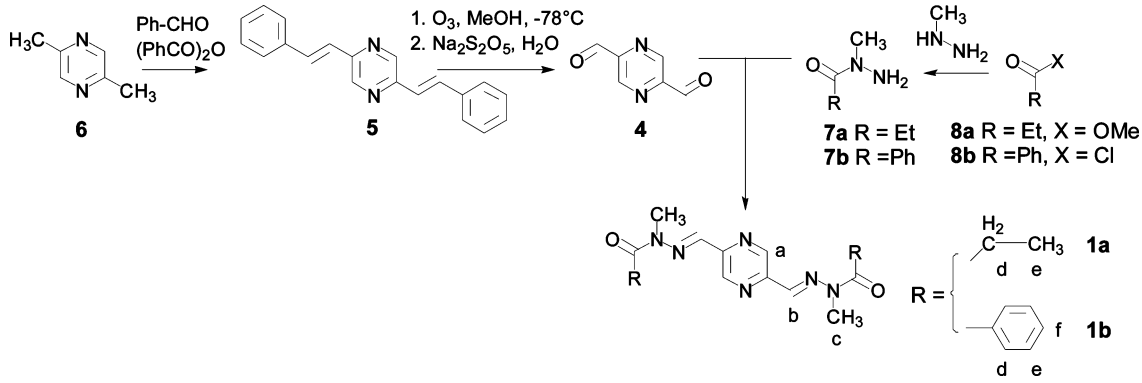

Experimental Section

General Procedures. Compounds 2,5-distyrylpyrazine[14] (**5**), pyrazine-2,5-dicarboxaldehyde[10] (**4**), benzoyl-N-methyl-hydrazide (**7a**),[12] and propionyl-N-methyl-hydrazide (**7b**)[10] were prepared as previously described. The following reagents were purchased from commercial sources: terpyridine (Aldrich), $Cu(OTf)_2$ (Fluka), $CDCl_3$ (Eurisotop).

NMR spectra were recorded on a Bruker AM 300 spectrometer. The solvent signal was used as an internal reference for ^{1}H NMR ($CHCl_3$, δ = 7.24 ppm) and ^{13}C NMR ($CHCl_3$ δ = 77.26 ppm) spectra. The following notation is used for the ^{1}H NMR spectral splitting patterns: singlet (s), doublet (d), triplet (t), and multiplet (m).

The 2D-NMR experiments used were correlation spectroscopy (COSY) and nuclear overhauser enhancement spectroscopy (NOESY).

Magnetic measurements were performed using a Quantum Design MPMS-XL SQUID magnetometer.

Mass spectra were recorded on a Bruker Microtof machine.

Synthetic Procedures. Pyrazine-2,5-dicarbaldehyde-bis(propionyl-N-methylhydrazone), 1a. Pyrazine-2,5-dicarboxaldehyde (193.7 mg, 1.423 mmol) and propionyl-N-methyl-hydrazide (290.7 mg, 2.846 mmol) were stirred in 35 mL of ethanol at 60 °C over 18 h. The precipitate was centrifuged, washed with ethanol, and dried under a vacuum. A yellowish solid resulted. Yield: 247 mg (57%). Mp: 228−229 °C. ^{1}H NMR ($CDCl_3$, 400 MHz, reference: solvent residual peak, δ 7.24 ppm): δ 9.11 (s, 2H); 7.76 (s, 2H); 3.39 (s, 6H); 2.90 (q, J = 7.5 Hz, 4H), 1.21 (t, J = 7.5 Hz, 6H) ppm. ^{13}C NMR ($CDCl_3$, 100 MHz, reference: solvent residual peak, δ 77.23 ppm): δ 176.24, 148.56, 141.18, 136.44, 28.31, 27.16, 9.47 ppm. HR-ES-MS (*m*/*z*): 311.1786 (calculated for $[M + Li]^+ = [C_{14}H_{20}N_6O_2Li]^+$: 311.1803).

Pyrazine-2,5-dicarbaldehyde-bis(benzoyl-N-methylhydrazone), 1b. Pyrazine-2,5-dicarboxaldehyde (99.6 mg, 0.732 mmol) and benzoyl-N-methyl-hydrazide (219.8 mg, 1.464 mmol) were stirred in 25 mL of ethanol at room temperature over 35 h. The precipitate was centrifuged, washed with ethanol, and dried under a vacuum. A yellowish solid resulted. Yield: 123 mg (42%). Mp: 282−283 °C. ^{1}H NMR ($CDCl_3$, 400 MHz, reference: solvent residual peak, δ 7.24 ppm): δ 8.69 (s, 2H), 7.77 (s, 2H), 7.68−7.66 (m, 4H), 7.48−7.24 (m, 6H), 3.56 (s, 6H) ppm. ^{13}C NMR ($CDCl_3$, 100 MHz, reference: solvent residual peak, δ 77.23 ppm): δ 176.24, 148.56, 141.18, 136.43, 28.31, 27.16, 9.47 ppm. HR-ES-MS (*m*/*z*): 407.1779 (calculated for $[M + Li]^+ = [C_{22}H_{20}N_6O_2Li]^+$: 407.1803).

Complex 9a, ($[Cu_2\mathbf{1a}(terpy)_2](OTf)_4$). A solution of ligand **1a** (24.9 mg, 0.0818 mmol) and $Cu(CF_3SO_3)_2$ (59.2 mg, 0.1636 mmol) in 2 mL of CH_3CN was stirred at 40 °C for 3 h. 2,2′;6′,2″-Terpyridine (38.1 mg, 0.1636 mmol) was added, and the solution thus obtained was stirred for 15 min at room temperature. Green crystals were grown by partial evaporation of the solvent at room temperature. They were filtered, washed with $CHCl_3$, and then dried under a vacuum. Yield: 50 mg (≈ 40%). Anal. calcd for **9a**·2$CHCl_3$ = $C_{50}H_{44}Cl_6Cu_2F_{12}N_{12}O_{14}S_4$: C, 34.65; H, 2.56; N, 9.70. Found: C, 34.45; H, 2.76; N, 9.85. HR-ES-MS (*m*/*z*): 1441.0772 (calcd. for $\{[Cu_2\mathbf{1a}(terpy)_2](OTf)_3\}^+ = \{C_{47}H_{42}Cu_2F_9O_{11}S_3\}^+$: 1441.0694).

Complex 9b, ($[Cu_2\mathbf{1b}(terpy)_2](OTf)_4$). A solution of ligand **1b** (12.3 mg, 0.0307 mmol) and $Cu(CF_3SO_3)_2$ (22.2 mg, 0.0614 mmol) in 3.3 mL of CH_3CN was stirred for 5 min at 50 °C. Then, $PhNO_2$ (1.9 mL) was added. Then, 2,2′;6′,2″-terpyridine (14.3 mg, 0.0614 mmol) was added, and the solution was stirred for 5 min at 50 °C. Green crystals were grown by partial evaporation of the solvent at room temperature. They were filtered, washed with $CHCl_3$, and then dried under a vacuum. Yield: 38 mg (≈78%). Anal. calcd for **9b** = $C_{56}H_{42}Cu_2F_{12}N_{12}O_{14}S_4$: C, 42.29; H, 2.66; N, 10.57. Found: C, 41.97; H, 2.93; N, 10.36. HR-ES-MS (*m*/*z*): 1439.0796 (calcd. for $\{[Cu_2\mathbf{1b}(terpy)_2](OTf)_3\}^+ = \{C_{55}H_{42}Cu_2F_9N_{12}O_{11}S_3\}^+$: 1439.0702).

Crystal Structure Determinations. Crystals suitable for X-ray crystallography were obtained by diffusion-recrystallization by using the appropriate solvent and nonsolvent, $CHCl_3/CH_3CN$ in the case of **1b**, or by evaporation of the solvent at room temperature for **9a** (solvent: CH_3CN) and **9b** (solvent: 1.75:1 $CH_3CN/PhNO_2$). The

(12) Hinman, R. L.; Fulton, D. *J. Am. Chem. Soc.* **1958**, *80*, 1895–1900.

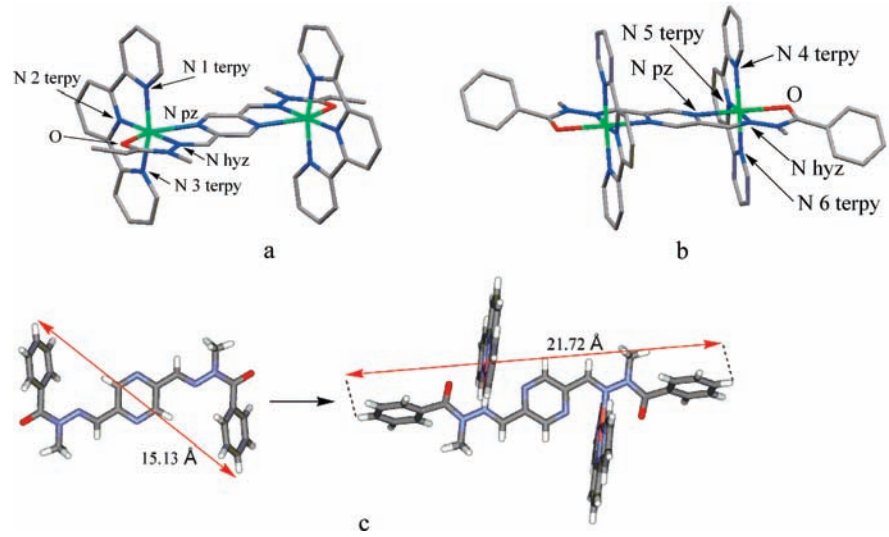

Figure 3. X-ray solid-state molecular structure of the rack complexes (a) **9a** and (b) **9b**. Hydrogens and anions are omitted for clarity. (c) The amplitude of the switch between the free ligand **1b** and its complex **9b** with respect to para protons is about 6.6 Å.

Table 1. Cu−A Distances (A = coordinating atom)

bond	length (Å)	
	9a	**9b**
Cu−O	2.275(3)	2.297(3)
Cu−N_{hyz}	2.034(3)	2.034(3)
Cu−N_{pz}	2.434(3)	2.283(3)
Cu−$N1_{terpy}$ or Cu−$N4_{terpy}$	2.039(3)	2.041(3)
Cu−$N2_{terpy}$ or Cu−$N5_{terpy}$	1.927(3)	1.918(3)
Cu−$N3_{terpy}$ or Cu−$N6_{terpy}$	2.039(3)	2.037(3)

Table 2. A−Cu−A Angles (A = Coordinating Atom)

9a		**9b**	
atoms	angle (deg)	atoms	angle (deg)
O−Cu−$N1_{terpy}$	95.66(12	O−Cu−$N4_{terpy}$	89.60(11)
O−Cu−$N2_{terpy}$	104.04(12)	O−Cu−$N5_{terpy}$	108.52(11)
O−Cu−$N3_{terpy}$	90.57(13)	O−Cu−$N6_{terpy}$	93.99(11)
O−Cu−N_{pz}	148.21(10)	O−Cu−N_{pz}	147.82(10)
O−Cu−N_{hyz}	73.79(12)	O−Cu−N_{hyz}	73.05(10)
$N1_{terpy}$−Cu−$N2_{terpy}$	80.23(13)	$N4_{terpy}$−Cu−$N5_{terpy}$	80.06(13)
$N1_{terpy}$−Cu−$N3_{terpy}$	160.49(13)	$N4_{terpy}$−Cu−$N6_{terpy}$	160.42(12)
$N2_{terpy}$−Cu−$N3_{terpy}$	80.33(14)	$N5_{terpy}$−Cu−$N6_{terpy}$	80.53(13)
$N1_{terpy}$−Cu−N_{pz}	92.80(12)	N_{pz}−Cu−$N4_{terpy}$	89.81(11)
$N2_{terpy}$−Cu−N_{pz}	107.50(12)	N_{pz}−Cu−$N5_{terpy}$	103.05(12)
$N3_{terpy}$−Cu−N_{pz}	91.55(12)	N_{pz}−Cu−$N6_{terpy}$	97.18(11)
$N2_{terpy}$−Cu−N_{hyz}	177.68(14)	N_{hyz}−Cu−$N4_{terpy}$	103.57(12)
$N1_{terpy}$−Cu−N_{hyz}	100.72(13)	N_{hyz}−Cu−$N5_{terpy}$	176.14(12)
$N3_{terpy}$−Cu−N_{hyz}	98.78(13)	N_{hyz}−Cu−$N6_{terpy}$	95.88(12)
N_{pz}−Cu−N_{hyz}	74.53(12)	N_{hyz}−Cu−N_{pz}	75.85(11)

crystals were placed in oil, and a single crystal was selected, mounted on a copper fiber, and placed in a low-temperature N_2 stream. Data were collected on a Nonius-Kappa-CCD diffractometer.

Ligand 1b. Formula, $C_{22}H_{20}N_6O_2$; formula weight, 400.44; crystal system:, monoclinic; space group, *C*2/*c* (No. 15). *a*, *b*, *c* [Å]: 26.4660(11), 6.2910(3), 12.0820(7). α, *β*, *γ* [deg]: 90, 104.7460(17), 90. V [Å^3] = 1945.37(17), *Z* = 4; D_{calcd} [g/cm^3] = 1.367; *μ*(Mo Kα) [mm^{-1}] = 0.092; F(000) = 840; crystal size [mm^3] = 0.10 × 0.14 × 0.16; *T* (K) = 173; radiation [Å] Mo Kα, 0.71073; *θ* min, max [deg] = 1.6, 28.7. Data set: −35/35, −7/8, −16/16. Tot., uniq. data, *R*(int): 4290, 2521, 0.039. Observed data with $I > 2\sigma(I)$: 1450. N_{ref}, N_{par}: 2521, 136. R, wR2, S: 0.0529, 0.1489, 0.99. Min. and max. resid. dens. [eÅ^{-3}]: −0.27, 0.22.

Complex 9a. Formula, $C_{28}H_{27}CuF_6N_8O_7S_2$; formula weight, 829.24; crystal system, triclinic; space group, $P\bar{1}$ (No. 2). *a*, *b*, *c* [Å]: 12.3870(4), 12.7180(4), 12.8450(5). α, *β*, *γ* [deg]: 63.7520(12), 89.2310(13), 79.1360(12). *V* [Å^3] = 1776.76(11); *Z* = 2; D_{calcd} [g/cm^3] = 1.550; *μ*(Mo Kα) [mm^{-1}] = 0.819; F(000) = 844; crystal size [mm^3] = 0.14 × 0.16 × 0.16; *T* (K) = 173; radiation [Å] Mo Kα, 0.71073; *θ* min, max [deg] = 1.7, 29.1. Data set: −16/16, −17/17, −17/17. Tot., uniq. data, *R*(int): 15189, 9466, 0.046. Observed data with $I > 2\sigma(I)$: 4943. N_{ref}, N_{par}: 9466, 469. R, wR2, S: 0.0547, 0.1745, 1.31. Min. and max. resid. dens. [eÅ^{-3}]: −0.86, 0.67.

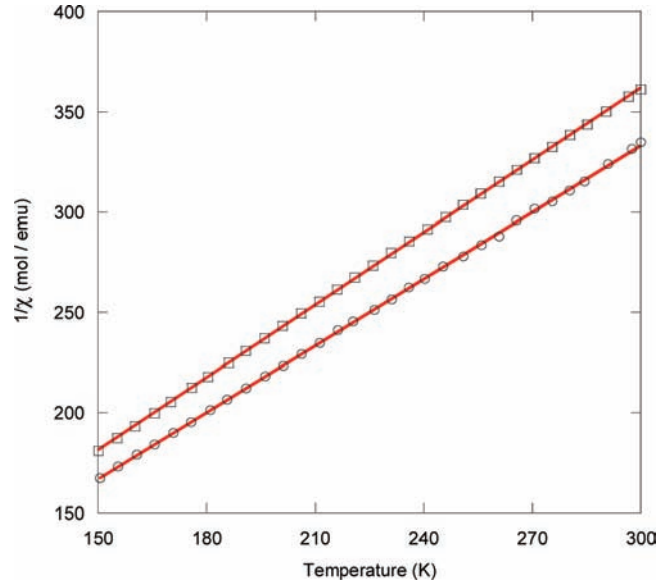

Figure 4. Curie−Weiss law $1/\chi = f(T)$ for complexes **9a** (○) and **9b** (□) (full lines = fit curves).

Complex 9b. Formula, $C_{62}H_{46}Cu_2F_{12}N_{13}O_{16}S_4$; formula weight, 1712.44; crystal system, triclinic; space group, $P\bar{1}$ (No. 2). *a*, *b*, *c* [Å]: 11.2710(2), 12.2970(2), 13.8230(3). α, *β*, *γ* [deg]: 76.8130(8), 85.3660(8), 66.7320(11). *V* [Å^3] = 1713.53(6); *Z* = 1; D_{calcd} [g/cm^3] = 1.660; *μ*(Mo Kα) [mm^{-1}] = 0.853; F(000) = 867; crystal size [mm^3] = 0.10 × 0.14 × 0.16; *T* (K) = 173; radiation [Å] Mo Kα, 0.71073. *θ* min, max [deg] = 3.2, 29.1. Data set: −15/14, −16/16, −18/18. Tot., uniq. data, R(int): 14303, 9148, 0.038. Observed data with $I > 2\sigma(I)$: 5756. N_{ref}, N_{par}: 9148, 505. R, wR2, S: 0.0717, 0.2047, 1.04. Min. and max. resid. dens. [eÅ^{-3}]: −0.75, 1.62.

CCDC-674125 (**1b**), CCDC-674126 (**9a**), and CCDC-674127 (**9b**) contain the supplementary crystallographic data for this paper.

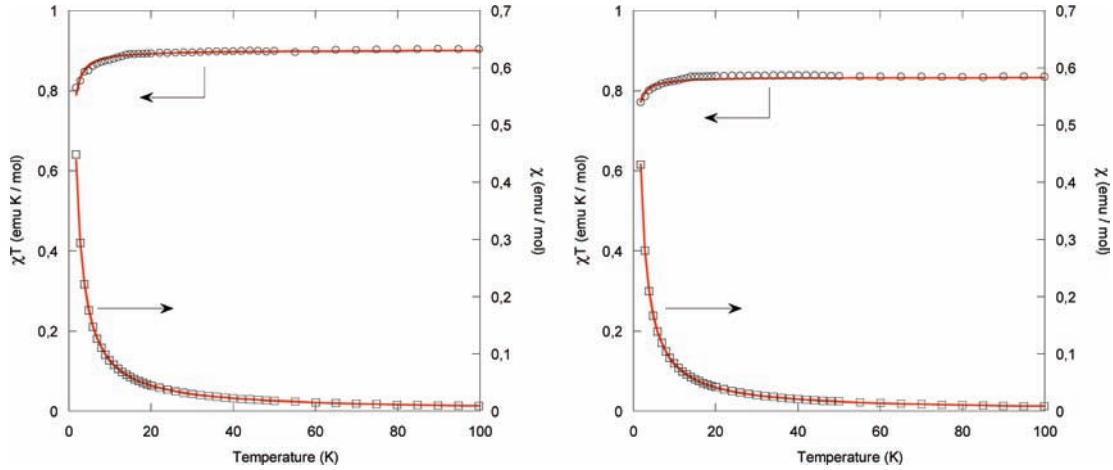

Figure 5. $\chi = f(T)$ (□) and $\chi T = f(T)$ (○) for complexes **9a** (left) and **9b** (right) (full lines = fit curves).

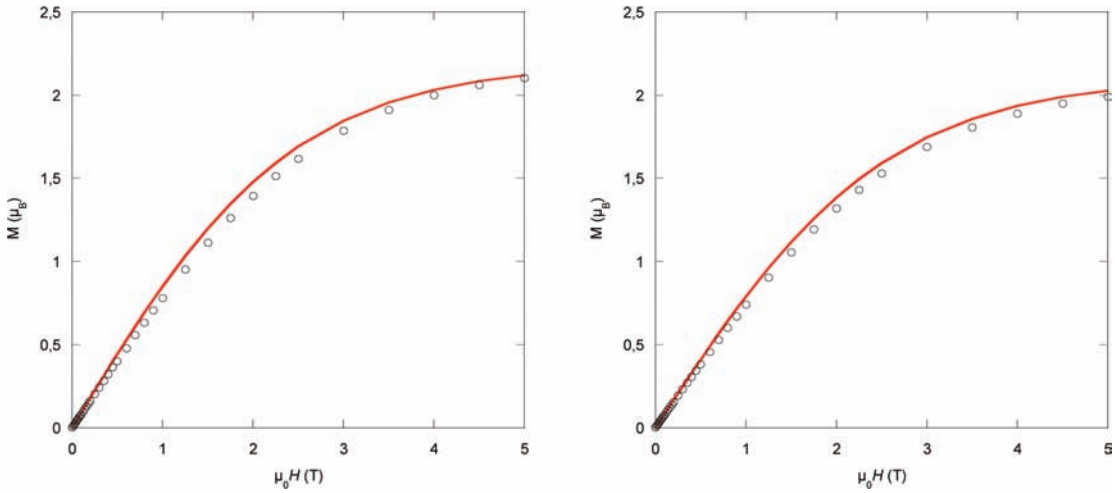

Figure 6. Magnetization vs field at 1.8 K for complexes **9a** (left) and **9b** (right). Open circles = experimental points, full lines = calculated curves using Brillouin's law (see text).

Table 3. Magnetic Parameters for the Rack-Type Complexes

	9a	**9a**
Curie constant C (emu K mol^{-1})	0.90	0.83
coupling constant J (cm^{-1})	−0.56(1)	−0.35(1)
g	2.19(1)	2.11(1)

These data can be obtained free of charge from the Cambridge Crystallographic Data Centre (www.ccdc.cam.ac.uk).

Results and Discussion

Ligand Synthesis and Structure. The hydrazide precursor **7** is obtained by a substitution reaction between methylhydrazine and the corresponding methyl-ester **8a**[12] or acylchloride **8b**.[13] The reaction of 2,5-dimethylpyrazine **6** with benzaldehyde and benzoic anhydride leads to 2,5-distyrylpyrazine[14] **5**, whose ozonolysis followed by reduction gives the pyrazine-2,5-dicarboxaldehyde[1a,10] **4**. The condensation of 2 equiv of hydrazide **7** with 1 equiv of dialdehyde **4**, in ethanol, at room temperature, yields the final ligand **1** (Scheme 2). Both compounds **4** and **7** are soluble in ethanol. Ligand **1** precipitates.

α,α′-Bypyridine adopts a *transoid* conformation[15] about the C−C bond connecting the two pyridine groups. The polyheterocyclic ligands containing this motif, as well as their hydrazone-based analogues, present the same property. For ligand **1**, the conformations around both OC−Nsp^3 and C_{hyz}−C_{pz} bonds are transoid, although the Npy_1 atoms from ligands **2** and **3** were replaced by the oxygen atom of the carbonyl group. Both the conformation (N−N bond, s-trans) and the configuration (N=C bond, *E*) of the hyz group in ligand **1** are similar to those of ligand **2**. These structural features were confirmed in the solid state by X-ray crystallography (Figure 3c) for ligand **1b**. The angle between the pyrazine and phenyl rings is about 60°.

The same holds in solution, as shown by 2D NMR (^{1}H−^{1}H NOESY) for ligands **1a** and **1b**. The key nuclear Overhauser effects are observed between the −CH_3 (proton c) and the hydrazone =CH− (proton b; for both ligands **1a** and **1b**)

(13) Wanner, M. J.; Koch, M.; Koomen, G.-J. *J. Med. Chem.* **2004**, *47*, 6875–6883.
(14) Hasegawa, M.; Asusuki, Y.; Susuki, F.; Nakanishi, H. *J. Polym. Sci., Part A: Polym. Chem.* **1969**, *7*, 743–752.
(15) (a) Merrit, L L., Jr.; Schroeder, E. D. *Acta Crystallogr.* **1956**, *9*, 801. (b) Bertinotti, F.; Liquori, A. M.; Pirisi, R. *Gazz. Chim. Ital.* **1956**, *86*, 893. (c) Nakamoto, K. *J. Phys. Chem.* **1960**, *64*, 1420. (d) Castellano, S.; Gunther, H.; Ebersole, S. *J. Phys. Chem.* **1965**, *69* (12), 4166. (e) Calder, I C.; Spotswood, T. M.; Tanzer, C. I. *Aust. J. Chem.* **1967**, *20* (6), 1195. (f) Barone, V.; Minichino, C.; Fliszar, S.; Russo, N. *Can. J. Chem.* **1988**, *66* (5), 1313. (g) Jaime, C.; Font, J. *J. Org. Chem. Med.* **1990**, *55* (9), 2637. (h) Howard, S. T. *J. Am. Chem. Soc.* **1996**, *118* (42), 10269.

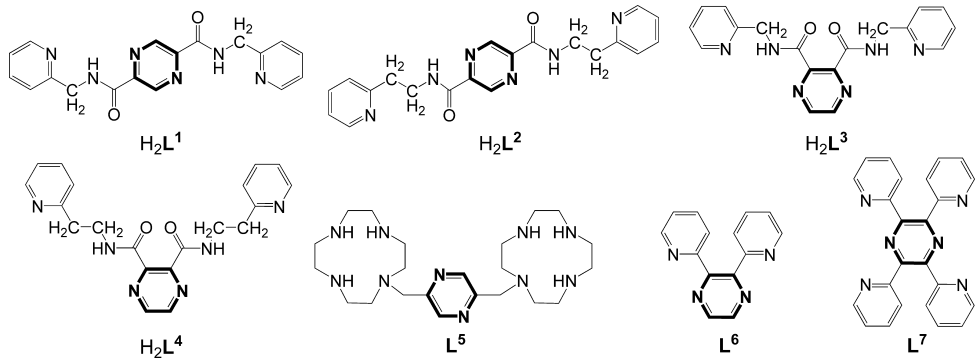

Figure 7. Structures of ligands $H_2\mathbf{L}^1-H_2\mathbf{L}^3$ and $\mathbf{L}^4$.

and between the $-CH_2-$ (proton d) of the Et group (ligand **1a**) or the C2 (and C6) protons (protons e) of the Ph group (ligand **1b**) and the pyrazine protons a (Scheme 2 and Figure 2; see also the Supporting Information).

Synthesis and Structure of the Rack-Type Complexes. The rack-like complexes were synthesized in a two-step, one-pot synthesis. The reaction of ligands **1** with 2 equiv of copper(II) triflate in acetonitrile for **1a** or in a MeCN/$PhNO_2$ mixture for **1b**, at 40−50 °C, leads to the dissolution of the ligand and the formation of the dinuclear complex $Cu_2\mathbf{1}(OTf)_4$ (not isolated), which reacts with 2 equiv of terpyridine to yield the rack-like complexes **9** ($[Cu_2\mathbf{1}(terpy)_2](OTf)_4$; Scheme 1). The complexes are obtained as crystals or microcrystalline powders by slow partial evaporation of their preparation solutions. The intermediate formation of the dinuclear complexes $Cu_2\mathbf{1}(OTf)_4$ was confirmed by ES-MS of the solution: the *m*/*z* calculated for $[Cu_2\mathbf{1a}(OTf)_3]^+ = [Cu_2(C_{14}H_{20}N_6O_2)(CF_3SO_3)_3]^+ = 876.8795$; that found was 876.8214. The *m*/*z* calculated for $[Cu_2\mathbf{1b}(OTf)_3]^+ = [Cu_2(C_{22}H_{20}N_6O_2)(CF_3SO_3)_3]^+ = 972.8795$; that found was 972.8632.

No attempts to synthesize the complexes starting directly from the three components (metal salt, terpy, and ligand **1**) were tried. However, it is interesting to note that the formation of these compounds is, in principle, competing with the formation of the [2 × 2] grid-like compound $[Cu_4\mathbf{1}_4](OTf)_8$ (or of a virtual polymeric species $[Cu_n\mathbf{1}_n](OTf)_{2n}$) and the complex $[Cu(terpy)_2](OTf)_2$. Indeed, the following equilibrium may be written:

$$[Cu_2\mathbf{1}(terpy)_2](OTf)_4 \rightleftarrows 1/n[Cu_n\mathbf{1}_n](OTf)_{2n} + [Cu(terpy)_2](OTf)_2$$

In the solid state, with respect to this equilibrium, only the rack was observed in the green crystals that were obtained. The bis(terpy) Cu(II) homocomplex has been previously described.[16] The X-ray structure of a polymeric assembly $[M_n\mathbf{L}_n](OTf)_{2n}$ was obtained in our laboratories (structure not shown), where M is Pb(II) and **L** is the homologue of **1a** where N−Me is replaced by N−H; so the existence of similar complexes of Cu(II) cannot be totally excluded. If $n = 4$, the formula corresponds to a [2 × 2] grid-like complex. ES-MS analysis of the preparation solution of the present complexes showed no peak corresponding to such a grid structure. Attempts to crystallize this grid alone were unfruitful (ligand **1a**; no crystal obtained) or resulted in the crystallization of the free ligand (in the case of **1b**). However, peaks corresponding to $[Cu(terpy)OTf]^+$ have been observed in solutions obtained by redissolving **9** in MeCN, this being explained by the dissociation of the rack in solution.

Although the thermodynamic properties of this kind of rack are not clearly established, it can be supposed that it represents the more likely structure.

The solid-state molecular structures of the two rack-like complexes were determined by X-ray crystallography (Figure 3a,b). They present an inversion center. The planes of the terpy units are almost perpendicular to the plane of the ditopic ligand (92.3° for the complex of **1a** and 92.8° for the complex of **1b**). The Cu−Cu average distance is 7.45 Å (7.59 in **1a** and 7.30 in **1b**). Each Cu(II) cation has a slightly distorted octahedral coordination geometry. The Cu(II) cations of a given rack are equivalent from a crystallographic point of view. The dihedral angle between the ligand plane and the phenyl ring in complex **9b** is 54°.

Binding of a metal ion to a hyz−pz unit of ligand **1** leads to a rotation around the C−C bond connecting the hyz and pz groups, and the same holds for the carbonyl−hyz unit, so that these two conformational changes from transoid to cisoid around the OC−Nsp^3 and $C_{hyz}-C_{pz}$ bonds generate the tridentate complexation subunit of the Cu(II) ion. Similar conformational changes occur in the terpy molecule upon the complexation of metal ions. These conformational changes correspond to variations in shape of significant amplitude. Thus, in the free ligand **1b**, the distance between the para protons of the phenyl rings is about 15.1 Å, and it increases to about 21.7 Å in the corresponding Cu(II) rack, an increase of around 6.6 Å (Figure 3c).

The length of the coordination bonds (see Table 1) can be arranged in the following way for the complex **9a**: $Cu-N2_{terpy} < Cu-N_{hyz} \approx Cu-N1_{terpy}$ and $Cu-3_{terpy} < Cu-O < Cu-N_{pz}$. For **9b**: $Cu-N2_{terpy} < Cu-N_{hyz} \approx Cu-N1_{terpy}$ and $Cu-3_{terpy} < Cu-N_{pz} < Cu-O$. The A−Cu−A angles (A = coordinating atom) are listed in Table 2.

Magnetic Susceptibility of the Complexes. Susceptibility measurements were performed in the temperature range 1.8−300 K with an applied field of 5 kOe. Field-dependent

(16) (a) Allmann, R.; Hevke, W.; Reinen, D. *Inorg. Chem.* **1978**, *17* (2), 378–382. (b) Alonso, C.; Ballester, L.; Gutierrez, A.; Perpinan, M. F.; Sánchez, A. E.; Azcondo, M. T. *Eur. J. Inorg. Chem.* **2005**, *486*, 495.

magnetization measurements at a given temperature confirm the absence of ferromagnetic impurities. Data were corrected for the sample holder, and diamagnetism was estimated from Pascal constants.

The rack-like complexes obey the Curie−Weiss law at high temperatures (Figure 4), with Curie constants $C = 0.90$ emu·K·mol^{-1} and 0.83 emu·K·mol^{-1} and Weiss temperatures $\theta = 0.12$ K and -0.29 K for racks of **1a** and of **1b**, respectively. The Curie constants are in very good agreement with what is expected for two Cu(II) ions. The Weiss temperatures are too small for their sign to be significant.

Actually, for both complexes, the χT product is almost constant at high temperatures and decreases below 50 K, which indicates the occurrence of antiferromagnetic interactions. Considering only an intramolecular interaction for each rack, the data were fit using the following spin Hamiltonian, where all parameters have their usual meaning and the spin operator **S** is defined as $\mathbf{S} = \mathbf{S}_{Cu1} + \mathbf{S}_{Cu2}$:

$$H = -J\mathbf{S}_{Cu1}\mathbf{S}_{Cu2} + g\beta\mathbf{HS}$$

In the present case, we did not need to consider any paramagnetic "impurity".

The fit (Bleaney−Bowers law)[17] leads to the following values for rack **9a**: $J = -0.56(1)$ cm^{-1} ($-0.81(1)$ K) and $g = 2.19(1)$, with an excellent agreement factor $R = 1.7 \times 10^{-5}$. Those for **9b** are: $J = -0.35(1)$ cm^{-1} ($-0.50(2)$ K) and $g = 2.11(1)$, with as well a very good agreement factor $R = 4 \times 10^{-5}$ (Figure 5), where $R = (\sum(\chi_{exp}T - \chi_{calcd}T)^2)/(\sum(\chi_{exp}T)^2)$.

The coupling constants are actually very weak. Therefore, the magnetization versus field curves at low temperatures (Figure 6) for both racks are logically not far from Brillouin's law for two spins, 1/2 using the same g values as obtained from the fit of the χT curves ($g = 2.19$ for rack **9a** and $g = 2.11$ for rack **9b**).

The magnetic parameters of the two racks are summarized in Table 3.

The results concerning J values are to be compared with the ones obtained for other copper(II) complexes containing pyrazine or pyrazine-derived ligands as backbone ligands. Magnetic interactions mediated by pyrazine-based bridging ligands are often considered to be weak and are generally antiferromagnetic.

The pyrazine-mediated superexchange was explained for pyrazine-bridged Cu(II) antiferromagnetic complexes $[Cu(pz)(NO_3)_2]_n$ ($J = -7.4$ cm^{-1})[18] by means of a π mechanism, involving the overlap of the b_{1g} and a_u ligand orbitals with the symmetric and antisymmetric combinations of the metal orbitals, d_s and d_a.

The dinuclear Cu(II) complex $[Cu_2(\mathbf{L}^1)(MeCN)_2(H_2O)_2](BF_4)_2 \cdot H_2O$ of the deprotonated diamide ligand *N*,*N*′-bis(2-pyridylmethyl)pyrazine-2,5-dicarboxamide, $H_2\mathbf{L}^1$ (Figure 7), exhibits very weak antiferromagnetic spin coupling ($J = -0.24$ cm^{-1}, $g = 2.2$), while the Cu(II) complex $[Cu_2(\mathbf{L}^2)(H_2O)_2(BF_4)_2] \cdot 2H_2O$ of its higher homologue *N*,*N*′-bis[2-(2-pyridyl)ethyl]-pyrazine-2,5-dicarboxamide, $H_2\mathbf{L}^2$ (Figure 7), exhibits very weak ferromagnetic spin coupling ($J = +0.67$ cm^{-1}, $g = 2.14$).[19a]

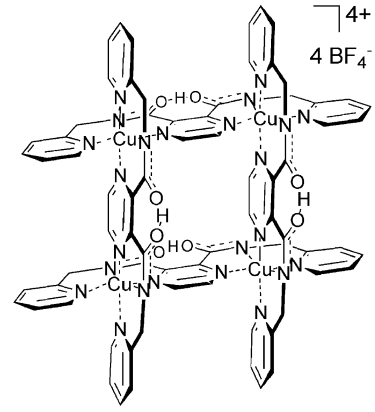

Figure 8. The [2 × 2] grid-like tetranuclear complex $[Cu_4(\mathbf{L}^3H)_4](BF_4)_4$ (ref 19b; reproduced by permission of The Royal Society of Chemistry).

The carbonyl groups in positions 2 and 3 correspond to *N*,*N*′-bis(2-pyridylmethyl)pyrazine-2,3-dicarboxamide ligand $H_2\mathbf{L}^3$ (Figure 7). The [2 × 2] grid-like tetranuclear complex obtained from the half-deprotonated ligand, $[Cu_4(\mathbf{L}^3H)_4](BF_4)_4 \cdot 3.5MeCN$[6h] (Figure 8) or $[Cu_4(\mathbf{L}^3H)_4](ClO_4)_4 \cdot 5CH_3OH \cdot 4H_2O$[20] is antiferromagnetic ($J = -5.87$ cm^{-1}, $g = 2.19$),[20] as well as the dinuclear complex $[Cu_2(\mathbf{L}^3H)(Cl_3)(H_2O)] \cdot H_2O$ ($J = -15.07$ cm^{-1}, $g = 2.17$).[20] Here also, in the dinuclear complex, the geometry of each Cu(II) ion is close to square-pyramidal, while in the grid, the coordination polyhedra are distorted octahedra, as is also the case for the rack-like complexes herein reported. Ab initio theoretical calculations[20] showed that, for the binuclear complex, the spin density of Cu(II) cations is located on the $d_{x^2-y^2}$ orbital, the superexchange involving this orbital and the N_{pz} atoms. It was also shown[20] that, in the [2 × 2] grid-like complex, the spin density is mainly located on one or more d orbitals and less on the N_{pz} atoms, a fact that diminishes the overlap with the pyrazine orbitals, as well as, consequently, the antiferromagnetic superexchange.[20] This result matches with the magnetic behavior of the rack-like complexes reported here, as the Cu(II) ions are in a N_5O distorted octahedral geometry.

Ligand $H_2\mathbf{L}^4$ (Figure 7), the ethylene analogue of $H_2\mathbf{L}^3$, produced two kinds of [2 × 2] grid-like complexes[19b] $[Cu_4(H_2\mathbf{L}^4)_2(H\mathbf{L}^4)_2](BF_4)_6 \cdot 4H_2O$ ($J = -1.9$ cm^{-1} and -2.4 cm^{-1}) and $[Cu_4(H\mathbf{L}^4)_4](BF_4)_4$ ($J = -3.02$ cm^{-1}), in both cases the coupling being antiferromagnetic.

The Cu(II) dinuclear complex of bis(cyclam)pyrazine ligand $\mathbf{L}^5$, $[Cu_2\mathbf{L}^5](ClO_4)_4$, has been found to have a weak value of the isotropic exchange interaction, attributed to poor spin delocalization toward the N atoms of the pyrazine ring.[19c]

(17) Bleaney, B.; Bowers, K. D. *Proc. R. Soc. London, Ser. A* **1952**, *214*, 451–465.
(18) Richardson, H. W.; Hatfield, W. E. *J. Am. Chem. Soc.* **1976**, *98*, 835–839.
(19) (a) Klingele, J.; Moubaraki, B. *Eur. J. Inorg. Chem.* **2005**, *1530*, 1541. (b) Klingele, J.; Boas, J. F.; Pilbrow, J. R.; Moubaraki, B.; Murray, K. S.; Berry, K. J.; Hunter, K. A.; Jameson, G. B.; Boyd, P. D. W.; Brooker, S. *Dalton Trans.* **2007**, 633−645. (c) El Ghachtouli, S.; Cadiou, C.; Déchamps-Olivier, I.; Chuburu, F.; Aplincourt, M.; Roisnel, T.; Turcry, V.; Patinec, V.; Le Baccon, M.; Handel, H. *Eur. J. Inorg. Chem.* **2008**, *30*, 4735–4744.
(20) Cati, D. S.; Ribas, J.; Ribas-Arino, J.; Stoeckli-Evans, H. *Inorg. Chem.* **2004**, *43* (3), 1021–1030.

For the dinuclear Cu(II) complex $[Cu_2(\mu\text{-}\mathbf{L}^6)(hfac)_4]$, where hfac = 1,1,1,5,5,5-hexafluoropentane-2,4-dionate and $\mathbf{L}^6$ = 2,3-bis(2-pyridyl)pyrazine (Figure 7), practically no magnetic interaction was observed between the two Cu(II) cations ($2J/k_B < 0.1$ K).[21] For a two-dimensional polymer *catena*-octakis(μ_2-acetato)[2,5-bis(2-pyridyl)pyrazine]tetracopper(II), an antiferromagnetic exchange mediated by the pyrazine-based ligand was observed ($J = -6.8$ cm^{-1}, $g = 2.23$).[22]

Cu(II) complexes of 2,3,5,6-tetrakis(2-pyridyl)pyrazine $\mathbf{L}^7$ (Figure 7) present antiferromagnetic exchange between two Cu(II) ions, likely involving the $\mathbf{L}^7$ pyrazine-based ligand, as in the following examples: $[Cu_2(\mu\text{-}\mathbf{L}^7)Cl_2](PF_6)_2$ ($J = -5.6$ cm^{-1}, $g = 2.16$),[23] $[Cu_2(\mu\text{-}\mathbf{L}^7)(N(CN)_2)_2(H_2O)](N(CN)_2)\cdot 3H_2O$ ($J = -43.7$ cm^{-1}, $g = 2.05$),[24] $[Cu_2(\mu\text{-}\mathbf{L}^7)Cl_4]\cdot 5H_2O$ ($J = -34.1$ cm^{-1}, $g = 2.05$),[25] $[Cu_2(\mu\text{-}\mathbf{L}^7)(H_2O)_4](ClO_4)_4$ ($J = -61.1$ cm^{-1}, $g = 2.13$),[25] and $[Cu_2(\mu\text{-}\mathbf{L}^7)Br_4]$ ($J = -40.9$ cm^{-1}, $g = 2.12$).[26] To explain the high J values,[25] it was assumed that the superexchange takes place through a σ mechanism, that is, the σ overlap between the two magnetic orbitals through the backbone pyrazine ring.

Conclusions

The new class of pyrazine-based ditopic bis(tridentate) ligands synthesized herein forms heteroleptic dinuclear rack-like Cu(II) complexes, presenting very weak pyrazine-mediated antiferromagnetic interactions. The introduction of appropriate substituents in the ligand molecule may allow for an increase and modulation of the superexchange. Also, longer rack complexes,[1] containing several cation centers, could yield systems presenting long-range interactions.

Acknowledgment. Juan Ramírez thanks CONACyT de Mexicò (registro 113226) for a predoctoral fellowship. We thank CNRS and AMNA European project for financial support. We thank Laurent Lévêque for CHN microanalyses. We thank Romain Carrière for MS analyses. We thank Lydia Brelot for help with X-ray crystallography.

Supporting Information Available: Additional figure and crystallographic information. This material is available free of charge via the Internet at http://pubs.acs.org.

IC801675D

(21) Ishida, T.; Kawakami, T.; Mitsubori, S.; Nogami, T.; Yamaguchi, K.; Iwamura, H. *J. Chem. Soc., Dalton Trans.* **2002**, *16*, 3177–3186.
(22) Neels, A.; Stoeckli-Evans, H.; Escuer, A.; Vicente, R. *Inorg. Chem.* **1995**, *34* (7), 1946–1949.
(23) Hadadzadeh, H.; Rezvani, A. R.; Yap, G. P. A.; Crutchley, R. J. *Inorg. Chim. Acta* **2005**, *358*, 1289–1292.
(24) Carranza, J.; Brennan, C.; Sletten, J.; Clemente-Juan, J. M.; Lloret, F.; Julve, M. *Inorg. Chem.* **2003**, *4226*, 8716–8727.
(25) Graf, M.; Stoeckli-Evans, H.; Escuer, A.; Vicente, R. *Inorg. Chim. Acta* **1997**, *257*, 89–97.
(26) Carranza, J.; Sletten, J.; Brennan, C.; Lloret, F.; Cano, J.; Julve, M. *Dalton Trans.* **2004**, *23*, 3997–4005.